Macrocyclic Mononuclear V^{IV} and V^{V}, Heterodinuclear $V^{IV}Ni^{II}$, and Heterotrinuclear $V^{IV}Ni^{II}V^{V}$ Complexes: Synthesis, Structure, Electrochemistry, and Magnetochemistry†

Kausik K. Nanda,[1a] Sasankasekhar Mohanta,[1a] Soma Ghosh,[1b] Monika Mukherjee,[1b] Madeleine Helliwell,[1c] and Kamalaksha Nag*,[1a]

Departments of Inorganic Chemistry and Solid State Physics, Indian Association for the Cultivation of Science, Calcutta 700 032, India, and Department of Chemistry, University of Manchester, Manchester M13 9PL, U.K.

Received July 28, 1994®

A macrocyclic tetramine–diphenol ligand (H_2L^2) with two different cavity sizes provided by an ethylene and propylene bridge, respectively, between the two sets of amine groups, on reaction with $VO(acac)_2$ produces a mixture of monomeric oxovanadium(IV) and -(V) complexes of the $[L^2]^{2-}$ anion. This mixture reacts with nickel(II) perchlorate and affords three compounds of composition $[(V^{IV}O)L^2Ni(H_2O)_2](ClO_4)_2$ (**4**), $[\{(V^{IV}O)L^2Ni(H_2O)\}\{(V^{V}O_2)(HL^2)\}](ClO_4)_2\cdot 3H_2O\cdot 2.5CH_3OH$ (**5**), and $[NiL^2(V^{IV}O)](ClO_4)_2$ (**6**). Complex **4** reacts with pyridine to produce $[(V^{IV}O)L^2Ni(py)](ClO_4)_2\cdot H_2O$ (**7**). The coordination geometry of nickel is octahedral in **4** and **5**, square planar in **6**, and square pyramidal in **7**. Vanadyl(IV) sulfate on reaction with H_2L^2 affords $[(V^{IV}O)(H_2L^2)(SO_4)]\cdot 5H_2O$ (**8**) as the sole product, in which both of the amino nitrogens of the $-NH(CH_2)_2NH-$ moiety are protonated. Complex **8** reacts with $Ni(acac)_2$ to produce $[NiL^2(V^{IV}O)(SO_4)]\cdot H_2O$ (**10**), in which the nickel is square planar. Complexes **4**, **6**, **7**, and **10** exhibit geometrical and positional isomerism. The cyclic voltammograms for **6**, **8**, $[(V^{IV}O)H_2L^2](NO_3)_2\cdot 2H_2O$ (**9**) and **10** exhibit a redox couple due to $V^{IV}O \rightarrow V^{V}O$ oxidation in all the cases. The six-coordinate oxovanadium complexes **8** and **10** undergo more facile oxidation ($E_{1/2}$ = 0.57 V vs Ag/AgCl) relative to the five-coordinate species **6** and **9** ($E_{1/2}$ = 0.80 V). Complexes **4**, **5**, and **7** behave ferromagnetically and the exchange coupling constants (J) for these compounds are as follows: 12 cm^{-1} (**4**); 2 cm^{-1} (**5**); 5 cm^{-1} (**7**). The crystal structure of the mixed-valence heterotrinuclear complex **5** has been determined. Crystal data for **5**: monoclinic; space group $P2_1/c$; a = 16.611(8) Å, b = 15.266(5) Å, c = 24.880(4) Å, β = 95.93(2)°, V = 6275(4) Å^3, Z = 4; R = 0.069, wR_2 = 0.183.

Introduction

The biochemistry of vanadium[2–4] has undergone considerable development in recent years. Concurrently, a resurgence of interest has occurred in the coordination chemistry of vanadium[5,6] in the oxidation states +3, +4, and +5. The binding of vanadium with tyrosine in transferrins,[7] the occurrence of polyphenol pigments in some vanadium accumulating aquatic organisms, tunicates[8] (order *Ascidiacea*), and the presence of V=O, V–O and V–N bonds in the active site of vanadium bromoperoxidases[9] isolated from several brown marine algae and a terrestrial lichen, which catalyze the formation of carbon–halogen bonds, have led to produce many interesting results with synthetic aryloxo (N,O-coordinated) vanadium complexes.[5,6,10–15]

Although a wide variety of vanadium complexes are now known, very few macrocyclic complexes have been reported so far.[16–18] We have recently reported[19] the chemistry of oxovanadium(IV) complexes derived from the dinucleating tetramine–diphenol macrocyclic ligand H_2L^1. Our study[20] with the dinickel(II) complexes of the related macrocyclic ligand H_2L^2, in which the cavity sizes of the two compartments of the ligand are not equal, has resulted the formation of mixed-spin state complexes. In these compounds the nickel(II) ion that occupies the smaller N_2O_2 cavity provided by the phenolic oxygens and $-NH(CH_2)_2NH-$ nitrogens obtains the low-spin (S = 0) square planar geometry, while the second nickel(II) ion occupying the larger N_2O_2 cavity provided by the phenolic

† This work is dedicated to Professor Animesh Chakravorty on the occasion of his 60th birthday.

® Abstract published in *Advance ACS Abstracts,* April 15, 1995.

(1) (a) Department of Inorganic Chemistry, IACS. (b) Department of Solid State Physicals, IACS. (c) University of Manchester.
(2) Chasteen, N. D., Ed. *Vanadium in Biological Systems*: *Physiology and Biochemistry*; Kluwer Academic Publishers: Dordrecht, The Netherlands, 1990.
(3) Wever, R.; Kustin, K. *Adv. Inorg. Chem.* **1990**, *35*, 81.
(4) Rehder, D. *Biometals* **1992**, *5*, 3.
(5) Rehder, D. *Angew. Chem., Int. Ed. Engl.* **1991**, *30*, 148.
(6) (a) Butler, A.; Carrano, C. J. *Coord. Chem. Rev.* **1991**, *109*, 61. (b) Butler, A.; Clague, M. J.; Meister, G. E. *Chem. Rev.* **1994**, *94*, 625.
(7) (a) Butler, A.; Eckert, H. *J. Am. Chem. Soc.* **1989**, *111*, 2802. (b) Chasteen, N. D.; Lord, E. M.; Thompson, H. J.; Grandy, J. K. *Biochim. Biophys. Acta* **1986**, *884*, 84. (c) Bertini, I.; Luchinat, C.; Messori, L. *J. Inorg. Biochem.* **1985**, *25*, 57.
(8) (a) Smith, M. J.; Kim, D.; Hornestein, B.; Nakanishi, K.; Kustin, K. *Acc. Chem. Res.* **1991**, *24*, 117. (b) Olta, E. M.; Bruening, R. C.; Smith, M. J.; Kustin, K.; Nakanishi, K. *J. Am. Chem. Soc.* **1988**, *110*, 6162.
(9) (a) Arber, J. M.; de Boer, E.; Garner, C. D.; Hasnain, S. S.; Wever, R. *Biochemistry* **1989**, *28*, 7968. (b) de Boer, E.; Van Kooyk, Y.; Tromp, M. G. M.; Plat, H.; Wever, R. *Biochim. Biophys. Acta* **1986**, *869*, 48.
(10) (a) Cornman, C. R.; Colpas, G. J.; Hoeschele, D.; Kampf, J.; Pecoraro, V. L. *J. Am. Chem. Soc.* **1992**, *114*, 9925. (b) Cornman, C. R.; Kampf, J.; Pecoraro, V. L. *Inorg. Chem.* **1992**, *31*, 1981.
(11) Vergopoulos, V.; Priebsch, W.; Fritzsche, M.; Rheder, D. *Inorg. Chem.* **1993**, *32*, 1844.
(12) (a) Carrano, C. J.; Nunn, M. C.; Quan, R.; Bonadies, J. A.; Pecoraro, V. L. *Inorg. Chem.* **1990**, *29*, 944. (b) Bonadies, J. A.; Butler, W. M.; Pecoraro, V. L.; Carrano, C. J. **1987**, *26*, 1218.
(13) (a) Karpishin, T. B.; Dewey, T. M.; Raymond, K. N. *J. Am. Chem. Soc.* **1993**, *115*, 1842. (b) Dewey, T. M.; Du Bois, J.; Raymond, K. N. *Inorg. Chem.* **1993**, *32*, 1729.
(14) (a) Neves, A.; Ceccatto, A. S.; Erasmus-Buhr, C.; Gehring, S.; Hasse, W.; Paulus, H.; Nascimento, O. R.; Batista, A. A. *J. Chem. Soc., Chem. Commun.* **1993**, 1782. (b) Neves, A.; Caccato, A. S.; Vencato, I.; Mascarenhas, Y. P.; Erasmus-Buhr, C. *J. Chem. Soc., Chem. Commun.* **1992**, 652.
(15) (a) Chakravarty, J.; Dutta, S.; Chandra, S. K.; Basu, P.; Chakravorty, A. *Inorg. Chem.* **1993**, *32*, 5343. (b) Chakravarty, J.; Dutta, S.; Chandra, S. K.; Basu, P.; Chakravorty, A. *Inorg. Chem.* **1993**, *32*, 4249.
(16) Comba, P.; Engelhardt, L. M.; Harrowfield, J. M.; Lawrance, G. A.; Martin, L. L.; Sargeson, A. M.; White, A. H. *J. Chem. Soc., Chem. Commun.* **1985**, 174.

0020-1669/95/1334-2861$09.00/0

oxygens and $-NH(CH_2)_3NH-$ nitrogens achieves the high-spin ($S = 1$) state with either octahedral or square pyramidal geometry. This observation has opened up a possibility to explore the chemistry of heterodinuclear nickel−vanadium complexes where the formation of positional isomers can be expected due to almost an equal probability for the two metal ions to occupy either of the ligand compartments. We report here the chemistry of isomeric heterodinuclear nickel(II)−oxovanadium(IV) complexes of the ligand H_2L^2, and structural characterization of the mixed-valence hetero-trinuclear complex $[\{(V^{IV}O)L^2Ni^{II}(H_2O)\}\{(V^VO_2)(HL^2)\}](ClO_4)_2 \cdot 3H_2O \cdot 2.5CH_3OH$.

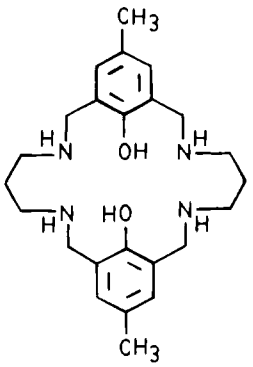

H_2L^1

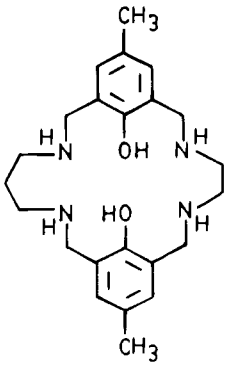

H_2L^2

Experimental Section

Materials. All chemicals were reagent grade and used as received. The ligand H_2L^2 was obtained as reported earlier.[20] Solvents were purified by standard methods.[21]

Physical Measurements. Infrared spectra were recorded on a Perkin-Elmer 783 spectrophotometer as KBr pellets and electronic spectra with a Shimadzu UV-160A or Hitachi U3400 spectrophotometer. X-Band EPR spectra were obtained on a Varian E-109C spectrometer using DPPH ($g = 2.0037$) as an external standard. Conductivity measurements were carried out using a Philips PR9500 conductivity bridge. The electrochemical measurements were performed at room temperature under O_2-free conditions using a BAS 100B electrochemical analyzer (Bioanalytical Systems). A three-electrode assembly (BAS) comprising a Pt working electrode, Pt auxiliary electrode, and a Ag/AgCl reference electrode was used. The supporting electrolyte was tetraethylammonium perchlorate (0.1 M) and all solutions were *ca.* 1 mM in complex. A PAR 155 vibrating sample magnetometer was used for susceptibility measurements at room temperature. Variable-temperature susceptibility measurements between 80 and 298 K were carried out by the Faraday method using a combination of Sartorius 4432 microbalance, Bruker B-E10C8 research magnet and B-VT 1000 temperature controller. Diamagnetic corrections were made using Pascal's constants. A Perkin-Elmer 240C elemental analyzer was used for microanalysis (C,H,N).

Synthesis of Complexes. $[(V^{IVO})L^2]$ (1), $[L^2(V^{IV}O)]$ (2), and $[(V^VO)(OH)L^2]$ (3). To a MeOH solution (100 mL) of H_2L^2 (2.0 g, 5 mmol) 1.32 g (5 mmol) of $VO(acac)_2$[22] dissolved in methanol (100 mL) was added over a period of 1 h. During addition an orange red product began to deposit. Stirring of the mixture in air was continued for 8 h, after which the product was collected by filtration and washed thoroughly with MeOH and $CHCl_3$; yield 2.25 g (95% based on the reactants). Recrystallization of the product, which actually is a mixture of three compounds (**1**−**3**), could not be carried out due to its very poor solubility in common organic solvents. Anal. Calcd for $C_{23}H_{32}N_4O_3V(VOL^2)$: C, 59.62; H, 6.91; N, 12.10; V, 11.00. Found: C, 59.03; H, 6.96; N, 11.81; V, 10.78.

$[(V^{IV}O)L^2Ni(H_2O)_2](ClO_4)_2$ (4), $[\{(V^{IV}O)L^2Ni^{II}(H_2O)\}\{(V^VO_2)(HL^2)\}](ClO_4)_2 \cdot 3H_2O \cdot 2.5CH_3OH$ (5), and $[NiL^2(V^{IV}O)](ClO_4)_2$ (6). To a stirred suspension of the mixture of compounds **1**−**3** (2.0 g) in MeOH (60 mL) was added $Ni(ClO_4)_2 \cdot 6H_2O$ (1.6 g). In a short while all the material dissolved, and a clear wine red solution was obtained, from which eventually a violet crystalline compound began to separate out. After 8 h the product (**4**) that deposited was collected by filtration and recrystallization from a MeCN−EtOH mixture; yield 1.1 g (34% based on VOL^2). Anal. Calcd for $C_{23}H_{36}N_4O_{13}Cl_2NiV$: C, 36.48; H, 4.76; N, 7.40. Found: C, 36.82; H, 4.72; N, 7.53.

The filtrate was allowed to evaporate slowly at room temperature when shining red crystals of **5** deposited over 2 d. These were collected by filtration and recrystallized from MeOH; yield 1.0 g (34%). Anal. Calcd for $C_{48.5}H_{83}N_8O_{21.5}Cl_2NiV_2$: C, 42.99; H, 6.13; N, 8.27. Found: C, 42.74; H, 6.08; N, 8.20.

The filtrate remaining thereafter was further concentrated to *ca.* 15 mL and mixed with 10 mL of EtOH. A pink microcrystalline material (**6**) that separated on standing was collected by filtration and recrystallized from a MeOH−Et_2O mixture; yield 0.2 g (7%). Anal. Calcd for $C_{23}H_{32}N_4O_{11}Cl_2NiV$: C, 38.31; H, 4.41; N, 7.77. Found: C, 38.56; H, 4.49; N, 7.85.

$[(V^{IV}O)L^2Ni(py)](ClO_4)_2 \cdot H_2O$ (7). Bright green crystals of (**7**) were obtained (80%) by diffusing Et_2O vapor into a solution of **4** in methanol-pyridine (1:1). Anal. Calcd for $C_{28}H_{39}N_5O_{12}Cl_2NiV$: C, 41.09; H, 4.77; N, 8.56. Found: 41.42; H, 4.88; N, 8.43.

$[(V^{IV}O)(H_2L^2)(SO_4)] \cdot 5H_2O$ (8). A MeOH solution (50 mL) of H_2L^2 (1.2 g, 3 mmol) was slowly treated with a solution of $VO(SO_4) \cdot xH_2O$ (0.50 g, 3 mmol) in MeOH (30 mL). The solution turned pink and was stirred for 1 h, after which it was rotary evaporated to *ca.* 15 mL and mixed with an equal volume of EtOH. On slow evaporation, pink crystals of **8** deposited, which were recrystallized from MeOH−MeCN (1:1) mixture; yield 1.2 g (60%). Anal. Calcd for $C_{23}H_{44}N_4O_{12}SV^-$: C, 42.36; H, 6.75; N, 8.59. Found: C, 42.05; H, 6.68; N, 8.67.

$[(V^{IV}O)(H_2L^2)](NO_3)_2 \cdot 2H_2O$ (9). A mixture of **8** (0.65 g, 1 mmol) and $Pb(NO_3)_2$ (0.33 g, 1 mmol) was stirred in MeOH (20 mL) for 0.5 h. The lead sulfate deposited was removed by filtration and the filtrate was reduced to *ca.* 5 mL when pink crystals of **9** deposited quantitatively. Anal. Calcd for $C_{23}H_{38}N_6O_{11}V$: C, 44.16; H, 6.08; N, 13.44. Found: C, 43.84; H, 6.16; N, 13.60.

$[NiL^2(V^{IV}O)(SO_4)] \cdot H_2O$ (10). A mixture of **8** (1.3 g, 2 mmol) and $Ni(acac)_2 \cdot H_2O$ (0.56 g, 2.2 mmol) in MeOH (60 mL) was stirred at room temperature. Initially a clear solution was obtained from which a microcrystalline compound began to separate out. After 2 h, the pink compound that deposited was filtered off and recrystallized from a CH_2Cl_2−MeOH (2:1) mixture; yield 0.9 g (70%). Anal. Calcd for $C_{23}H_{34}N_4O_8SNiV$: C, 43.42; H, 5.35; N, 8.81. Found: C, 43.11; H, 5.27; N, 8.69.

Conversion of 10 to 6. Quantitative conversion of **10** to **6** was accomplished by treating a suspension of **10** in MeOH with a molar equivalent of $Ba(ClO_4)_2 \cdot 3H_2O$, followed by filtration and evaporation of the filtrate.

X-ray Structure Determination. Single crystals of $[\{(V^{IV}O)L^2Ni^{II}(H_2O)\}\{(V^VO_2)(HL^2)\}](ClO_4)_2 \cdot 3H_2O \cdot 2.5CH_3OH$ (**5**) were grown by slow evaporation of a methanol solution of the compound. X-ray data were collected on a Rigaku AFC5R diffractometer with graphite monochromated Cu Kα radiation using $\omega-2\theta$ scan mode. Crystallographic details are given in Table 1. The unit cell dimensions were obtained by least-squares refinement of 20 automatically centered reflections. During data collection 3 standard reflections monitored after every 150 indicated a decay of 7% and this was corrected for Lorentz−polarization effects and for absorption (transmission factors varied between 0.6679 and 1.0) by an emperical method.[23] A total of 10 110 reflections were collected in the range $2\theta = 4-110°$, with $h = 0-18$, $k = 0-17$ and $l = \pm 27$, of which 5139 independent reflections with $I > 3\sigma(I)$ were used for structure determination. Neutral atom

(17) (a) Knopp, P.; Wieghardt, K.; Nuber, B.; Weiss, J.; Sheldrick, W. S. *Inorg. Chem.* **1990**, *29*, 363. (b) Knoppen, M.; Fresen, G.; Wieghardt, K.; Llusar, R. M.; Nuber, B.; Weiss, J. *Inorg. Chem.* **1988**, *27*, 721. (c) Wieghardt, K.; Bossek, V.; Volckmar, K.; Swiridoff, W.; Weiss, J. *Inorg. Chem.* **1984**, *23*, 1387.
(18) Dutton, J. C.; Fallon, G. D.; Murray, K. S. *J. Chem. Soc., Chem. Commun.* **1990**, 64.
(19) Das, R.; Nanda, K. K.; Mukherjee, A. K.; Mukherjee, M.; Heliwell, M.; Nag, K. *J. Chem. Soc., Dalton Trans.* **1993**, 2241.
(20) Nanda, K. K.; Das, R.; Venkatsubramanian, K.; Paul, P.; Nag, K. *J. Chem. Soc., Dalton Trans.* **1993**, 2515.
(21) Perrin, D. D.; Armarego, W. L. F.; Perrin, D. R. *Purification of Laboratory Chemicals*, 2nd ed.; Pergamon: Oxford, England, 1986.
(22) Rowe, R. A.; Jones, M. M. *Inorg. Synth.* **1957**, *5*, 113.

Table 1. Crystallographic Data for $[\{(V^{IV}O)L^2Ni^{II}(H_2O)\}\{(V^VO_2)(HL^2)\}](ClO_4)_2{\cdot}3H_2O{\cdot}2.5CH_3OH$ (**5**)

formula	$C_{46}H_{65}N_8O_{15}Cl_2NiV_2{\cdot}4H_2O.2{\cdot}5CH_3OH$	V, Å^3	6275(4)
fw	1353.72	Z	4
cryst size, mm	0.25 × 0.20 × 0.10	D_{calcd}, g cm^{-1}	1.433
cryst syst	monoclinic	λ(CuKα), Å	1.5418
space group	$P2_1/c$	μ, cm^{-1}	42.4
a, Å	16.611(8)	temp, K	296
b, Å	15.266(5)	F(000)	2840
c, Å	24.880(4)	R[a]	0.069
β, deg	95.93(2)	wR_2[b]	0.183

[a] $R = [\sum||F_o| - |F_c||/\sum|F_o|]$ for $F_o > 4\sigma(F_o)$. [b] $wR_2 = [\sum w(F_o^2 - F_c^2)^2/\sum w(F_o^2)^2]^{1/2}$ where $w = 1/[\sigma^2(F_o^2) + (0.0975P)^2 + 20.15P]$ and $P = (F_o^2 + 2F_c^2)/3$.

scattering factors used were those of Cromer and Waber.[24] The structure was solved by the Patterson heavy-atom method and refined by full-matrix least-squares techniques using the program SHELXS-86.[25] The position of the remaining non-hydrogen atoms and a few solvent molecules were located by weighted Fourier synthesis. Isotropic refinement of the non-hydrogen atoms followed by successive difference Fouriers indicated positions of the remaining solvent molecules. All solvent molecules, except OW(1), are highly disordered and were treated isotropically with fixed site occupancy factors, while the non-hydrogen atoms along with OW(1) were refined anisotropically. The hydrogen atoms (excepting those belongong to the solvent molecules) were placed at the geometrically calculated positions with fixed isotropic thermal parameters. The final least-squares refinement based on F^2, using the program SHELXL-93,[26] converged to $R = 0.0691$ and $wR_2 = 0.1826$. The number of parameters refined were 752, and the maximum fluctuations in the final ΔF map were in the range +0.84 to −0.34 e Å^{-3}. All calculations were performed with a VAX 3400 computer.

Results and Discussion

Synthesis, Characterization, and Isomerism. The macrocyclic ligand H_2L^2 reacts almost quantitatively with $VO(acac)_2$ in the presence of air to produce an orange red material whose composition approaches closely to that of VOL^2 and which is practically insoluble in all common organic solvents, including *N,N'*-dimethylformamide and dimethyl sulfoxide. Characterization of this material turned out to be difficult because owing to the solubility problem UV−vis, NMR and EPR spectra could not be recorded. The room temperature magnetic moment (ca. 1.4 μ_B at 300 K) is indicative of the presence of a mixture of vanadium(IV) and -(V) species and/or a strongly antiferromagnetically coupled oxovanadium(IV) complex. The IR spectrum shows characteristic ligand N−H stretching vibrations at 3270 and 3230 cm^{-1} and the NH bending vibration at 1610 cm^{-1}. A medium intensity band observed at 3120 cm^{-1}, which is absent in the free ligand, can be associated to a metal-bound OH stretch. Furthermore, the two bands observed at 945 and 860 cm^{-1} (Table 2) provides evidence in favor of the presence of terminal V=O stretch and a V=O stretch expected for bridging V = O··X (X = V, H etc.) moiety, respectively. Thus, on the basis

Scheme 1[a]

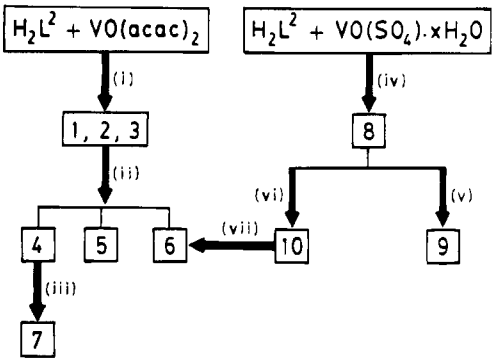

[a] Key: (i) MeOH; (ii) $Ni(ClO_4)_2{\cdot}6H_2O$; (iii) pyridine; (iv) MeOH; (v) $Pb(NO_3)_2$; (vi) $Ni(acac)_2{\cdot}H_2O$; (vii) $Ba(ClO_4)_2{\cdot}3H_2O$.

of the elemental analysis, magnetic moment, and IR data the presence of $[V^{IV}OL^2]$ and $[V^VO(OH)L^2]$ species in the orange red material is suspected. This receives support from the following chemical reactivity. As shown in Scheme 1 the material, despite its poor solubility, reacts smoothly with nickel(II) perchlorate in methanol to produce three different compounds, **4**−**6**, whose formation can be rationalized only by considering that the precursor material is also a mixture of three different species, viz. **1**−**3**. It will become evident that **1** and **2** are the isomeric vanadium(IV) complexes of composition $[VOL^2]$, which differ with respect to the ligand compartment occupancy, while **3** is a vanadium(V) complex whose composition can be considered as $[VO(OH)L^2]$. Oligomeric V=O··V=O·· interactions[27] in these species can be held responsible for their poor solubility behavior.

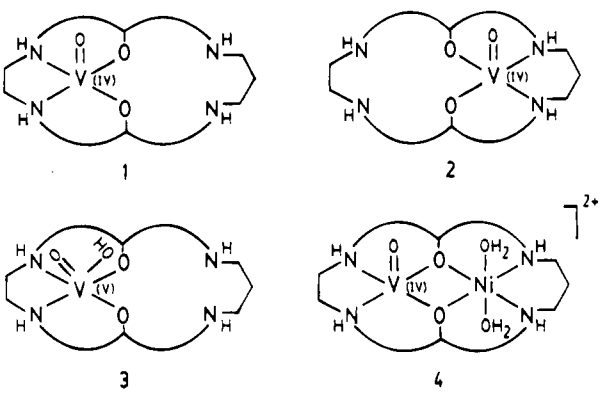

A few IR and electronic spectral data for the complexes are given in Table 2. The IR spectra of complexes **4**−**6** show features due to the ligand NH stretchings (3270−3200 cm^{-1}) and bending (1610 cm^{-1}) and uncoordinated perchlorate anions (1100 and 630 cm^{-1}). While the occurrence of two NH

Table 2. Electronic and IR Spectral Data for the Complexes

complex	λ_{max}, nm(ϵ, M^{-1} cm^{-1})	ν, cm^{-1}
1−**3**		3270 w, 3230 w (ν_{NH}); 3120 m (ν_{OH});1610 m (δ_{NH}); 945 s, 860 s ($\nu_{V=O}$)
4	1150 (6), 765 (30), 520 (55), 370 (400), 290 (12 500)[a]	3270 w, 3240 w (ν_{NH}); 1610 m (δ_{NH}); 1100 s, 630 m ($\nu_{ClO_4^-}$); 965 ($\nu_{V=O}$)
5	1100 (5), 500 (2400), 375 (3250), 290 (13 600)[b]	3270 w, 3230 w, 3200 w (ν_{NH}); 1610 m (δ_{NH}); 1100 s, 630 m ($\nu_{ClO_4^-}$); 960 s, 865 s, 855 m ($\nu_{V=O}$)
6	760 (40), 510 (325), 295 (14 000)[c]	3260 w, 3230 w (ν_{NH}); 1610 m (δ_{NH}); 1100 s, 630 m ($\nu_{ClO_4^-}$) 970 ($\nu_{V=O}$)
7	1400 (15), 770 (25), 610 (35), 515 (60), 380 (430)[d]	3240 m (ν_{NH}); 1620 m (δ_{NH}); 1600 m, 750 s, 700 s (py-ring) vibr); 1100 s, 630 m ($\nu_{ClO_4^-}$); 970 s ($\nu_{V=O}$)
8	795 (35), 510 (130), 295 (11 100)[a]	3250 w, 2850 w, 2760 w (ν_{NH}); 1615 m (δ_{NH}); 1170 m, 1130 s, 1045 m, 630 sh, 620 m ($\nu_{SO_2^{2-}}$); 950 s ($\nu_{V=O}$)
9	780 (30), 510 (120), 295 (10 300)[b]	3260 w, 3230 w, 2860 w, 2750 w (ν_{NH}); 1620 (δ_{NH}); 1380 s, 1080 m, 835 s ($\beta_{NO_3^-}$); 970 s ($\nu_{V=O}$)
10	760 (40), 490 (120), 370 sh, 270 (10 500)[b]	3250 m (ν_{NH}); 1620 (δ_{NH}); 1160 s, 1120 s, 1065 m, 625 m, 610 m ($\nu_{SO_4^{2-}}$); 955 s ($\nu_{V=O}$)

[a] In MeCN. [b] In MeOH. [c] In MeOH−MeCN. [d] In MeOH−pyridine.

stretchings in the heterodinuclear complexes **4** and **6** are indicative of the presence of two sets of NH groups coordinated to two different metal ions, an additional ν(NH) vibration observed in the heterotrinuclear complex **5** can be related to the uncoordinated NH nitrogens in this compound. An insight regarding the types of the vanadyl groups present has been obtained by comparing the V=O stretching energies of the complexes. As expected both **4** and **6** exhibit a terminal ν(V=O) between 970 and 960 cm^{-1}, while complex **5** exhibits in addition to the $\nu(V{=}O_{tr})$ at 960 cm^{-1} a pair of bands at 865 and 855 cm^{-1}. These two lower energy bands are most likely due to V=O stretchings in V=O··V and V=O··Ni.

The known electronic spectral features of the dinickel(II) complexes of H_2L^2 have been quite helpful to characterize the heteronuclear nickel–vanadium complexes. We previously noted[20] that in the mixed spin-state complex $[Ni_2L^2(H_2O)_2](ClO_4)_2$ the metal ion occupying the smaller ligand compartment (derived from the $-NH(CH_2)_2NH-$ unit) is square planar and does not undergo stereochemical change, while the high-spin six-coordinate nickel(II) occupying the larger compartment (derived from $-NH(CH_2)_3NH-$ unit) transforms to square pyrimidal geometry when the coordinated aqua molecules are replaced by neutral nitrogen donors, such as pyridine. The electronic spectrum of $[(V^{IV}O)L^2Ni^{II}(H_2O)_2](ClO_4)_2$ (**4**) exhibits a broad band of weak intensity around 1100 nm and three more bands of increasing intensities at 765, 520, and 370 nm. Among these, while the bands at 1150 and 375 nm can be reasonably attributed to $^3A_{2g} \rightarrow {}^3T_{2g}$ and $^3A_{2g} \rightarrow {}^3T_{1g}(P)$ transitions in octahedral nickel(II), as also the band at 765 nm due to $d_{xy} \rightarrow d_{yz}, d_{zx}$ transition in oxovanadium(IV), the remaining band at 520 nm seems to arise due to superposing $^3A_{2g} \rightarrow {}^3T_{1g}(F)$ and $d_{xy} \rightarrow d_{x^2-y^2}$ transitions of both the metal centers. Thus, in complex **4** the nickel atom must be occupying the larger compartment of the ligand. Moreover, **4** on treatment with pyridine produces $[(V^{IV}O)L^2Ni^{II}(py)](ClO_4)_2$ (**7**), in which the lowest energy d–d band is shifted to 1400 nm with an appreciable increase in intensity, a feature typical of square pyramidal nickel(II) complexes.[28] It may be noted that complex **7** exhibits five absorption maxima in the visible region, of which the bands at 1400, 610, and 380 nm are assignable to $^3B_1 \rightarrow {}^3E(F)$, $^3B_1 \rightarrow {}^3E(P)$, and $^3B_1 \rightarrow {}^3A_2(P)$ transitions, respectively, for high-spin square pyramidal nickel(II). We note that we have already observed similar stereochemical conversion from octahedral to square pyramidal geometry in the dinickel(II) complexes of both H_2L^1 and H_2L^2 and reported[20,29] their structures. Clearly, **4** and hence **7** owe their origin to **1**.

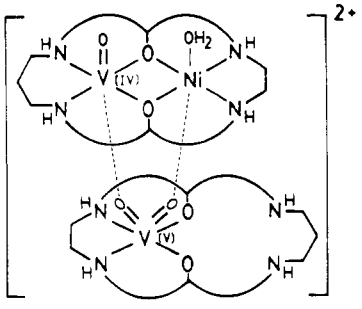

5

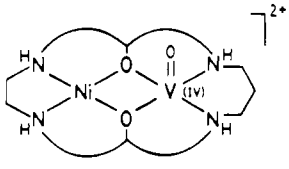

6

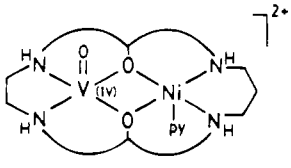

7

The formation of the mixed-valence heterotrinuclear complex, $[\{(V^{IV}O)L^2Ni^{II}(H_2O)\}\{(V^VO_2)(HL^2)\}](ClO_4)_2$·solvent (**5**), has been structurally verified. The room temperature magnetic moment of this compound (3.97 μ_B), indicates a spin state of $S = {}^3/_2$ and is compatible with the above formulation. As will be seen, the nickel atom occupying the smaller ligand compartment achieves an octahedral geometry, in contradiction to the expected square planar geometry, through the coordination of a water molecule and an oxygen atom of the $\{(V^VO_2)(HL^2)\}$ moiety. The $[\{(VO)L^2Ni(H_2O)\}\{(VO_2)(HL^2)\}]^{2+}$ cation is stable in solution since a characteristic d–d band due to octahedral nickel(II) is observable at 1100 nm. Another important spectral feature of this compound is the occurrence of an intense band with the peak at 500 nm (ϵ = 2400 M^{-1} cm^{-1}), which is most likely due to intervalence charge transfer transition. Apparently, in the absorption enclave of this band at the lower energy range some other additional spectral features have got submerged. The genesis of **5** can be logically traced back to the presence of species **2** and **3** in the insoluble reaction product of H_2L^2 and $VO(acac)_2$. The conversion of $[V^VO(OH)L^2]$ to *cis*-$[(V^VO_2)HL^2]$ occurs through a coordination induced proton transfer reaction.

The third complex that has been isolated by reacting the mixture of **1**–**3** with nickel(II) perchlorate is $[Ni^{II}L^2(V^{IV}O)](ClO_4)_2$ (**6**). This compound is EPR-active (1.82 μ_B at 300 K) and exhibits an isotropic eight-line spectrum in MeOH with g_{iso} = 1.973 and A_{iso} = 0.0089 cm^{-1} at 295 K. The EPR spectrum is attributable to a single $S = {}^1/_2$ species in which the unpaired electron in a d_{xy} orbital is coupled to the nuclear spin of the vanadium nucleus ($I = {}^7/_2$). The electronic spectrum of the complex exhibits its lowest energy band at 760 nm evidently due to the $d_{xy} \rightarrow d_{yz}, d_{xz}$ transition of vanadium(IV), while a second band at 510 nm seems to be due to a combination of transitions occuring at the vanadium center ($d_{xy} \rightarrow d_{x^2-y^2}$) and square planar nickel(II) center.

When H_2L^2 is reacted with vanadyl(IV) sulfate, $[(V^{IV}O)(H_2L^2)(SO_4)]\cdot 5H_2O$ (**8**) is obtained exclusively. The composition of **8** indicates that two of the secondary amines are protonated to maintain electrical neutrality of the complex. This is verified by observing a large shift of NH stretching frequencies of the protonated amines to lower energies (2850 and 2760 cm^{-1}) relative to the coordinated amines (3250 cm^{-1}). Moreover, the splitting of $\nu_3[SO_4^{2-}]$ (1170, 1130, and 1045 cm^{-1}) and $\nu_2[SO_4^{2-}]$ (630 and 620 cm^{-1}) provides a clear indication of the coordinated sulfate. The terminal V=O stretching occurs at 950 cm^{-1}. The EPR spectrum of **8** in MeOH at room temperatures has the features (g_{iso} = 1.976, A_{iso} = 0.0088 cm^{-1}) expected for a mononuclear oxovanadium(IV) complex with a N_2O_4 coordination environment.[5] All these observations are consistent with the recently reported[30] structure (shown in Figure 1) of **8**. It may be noted that the vanadium occupies the N_2O_2 equatorial plane provided by the larger compartment of the

(23) North, A. C. T.; Phillips, D. C.; Mathews, F. S. *Acta Crystallogr., Sect. A* **1968**, *24*, 351.
(24) Cromer, D. T.; Waber, J. T. *International Tables for X-ray Crystallography*; The Kynoch Press: Birmingham, England, 1974; Vol. IV.
(25) Sheldrick, G. M. SHELXS-86 A Program for Crystal Structure Determination. University of Gottingen, Germany, 1986.
(26) Sheldrick, G. M. SHELXL-93 A Program for Crystal Structure Refinement, Gamma-Test Version. University of Gottingen, Germany, 1993.
(27) Drake, R. F.; Crawford, V. H.; Hatfield, W. E.; Simpson, G. D.; Carlisle, G. O. *J. Inorg. Nucl. Chem.* **1975**, *37*, 291.
(28) Lever, A. B. P. *Inorganic Electronic Spectroscopy*, 2nd ed.; Elsevier: Amsterdam, 1984.
(29) Nanda, K. K.; Das, R.; Newlands, M. J.; Hynes, R.; Gabe, E. J.; Nag, K. *J. Chem. Soc., Dalton Trans.* **1992**, 897.
(30) Ghosh, S.; Mukherjee, M.; Mukherjee, A. K.; Mohanta, S.; Heliwell, M. *Acta Crystallogr., Sect. C* **1994**, *50*, 1204.

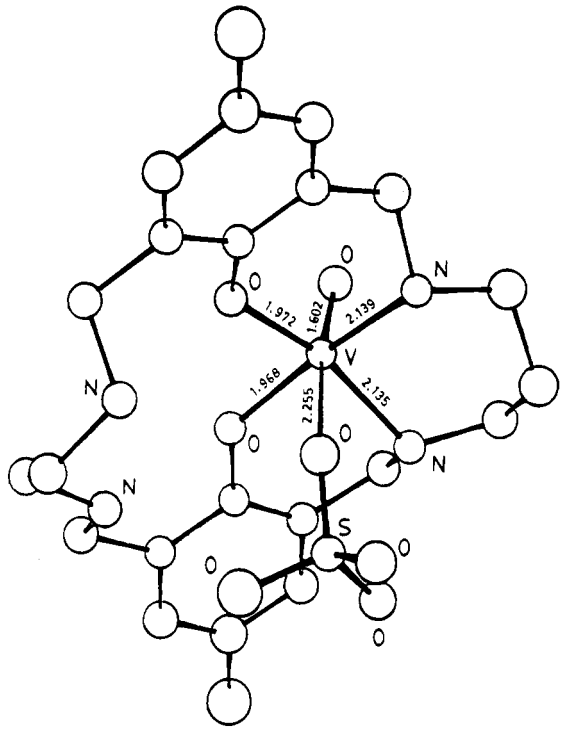

Figure 1. Perspective view of $[(VO)(H_2L^2)(SO_4)]\cdot 5H_2O$ (**8**).

ligand and due to the significant *trans* influence of the vanadyl oxygen and V−O(sulfate) distance is appreciably long, 2.225 Å.

Complex **8** quantitatively transforms to the nitrate salt **9** on treatment with lead nitrate. It appears that the vanadium(IV) center in **9** has a 5-fold coordination geometry because in MeCN it behaves as a 1:2 electrolyte ($\Lambda = 230\ \Omega^{-1}\ cm^2\ M^{-1}$), and in the solid state the IR spectrum shows bands due to the ionic nitrate at 1380, 1080, and 835 cm^{-1}.

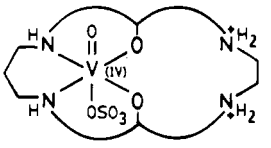

8

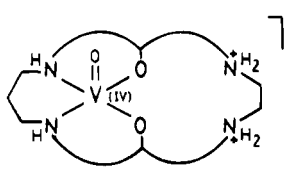

9

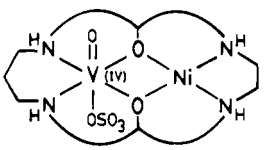

10

The insertion of a nickel(II) ion into the vacant ligand compartment of **8** cannot be carried out straightforwardly. However, when **8** is reacted with 1 equiv of $Ni(acac)_2$, nickel smoothly gets introduced according to eq 1 producing **10**, which

$$[VO(H_2L^2)(SO_4)] + Ni(acac)_2 \rightarrow [NiL^2(VO)(SO_4)] + 2Hacac \quad (1)$$

is a nonelectrolyte with the expected square planar geometry for the nickel atom. The EPR spectra of the mononuclear oxovanadium(IV) complex **8** and the heterodinuclear oxovanadium(IV)-nickel(II) complex **10** are very similar in CH_2Cl_2−MeOH solution both at room temperature and at 77 K. The frozen solution spectrum of **10** shown in Figure 2 is characterized by an axial symmetry of two sets of eight lines with the following spin-Hamiltonian parameters: $g_{\|} = 1.954$, $g_{\perp} = 1.982$, $A_{\|} = 0.0164\ cm^{-1}$, and $A_{\perp} = 0.0053\ cm^{-1}$.

The removal of the coordinated sulfate in **10** by $Ba(ClO_4)_2$ provides an alternative, unambiguous pathway for generating complex **6**. It may be noted that the heterodinuclear complexes **4**, **6**, **7**, and **10** are an unique combination of positional and geometrical isomers which, to our knowledge, have no precedence in macrocyclic systems of this sort.

Structure of 5. A perspective view of the mixed-valence heterotrinuclear $[\{(V^{IV}O)L^2Ni^{II}(H_2O)\}\{(V^{V}O_2)(HL^2)\}]^{2+}$ cation is shown in Figure 3. The atomic coordinates and isotropic thermal parameters are given in Table 3, while bond distances and angles pertaining to the metal coordination spheres are given in Table 4.

The two metal centers in the heterodinuclear $\{(VO)L^2Ni(H_2O)\}^{2+}$ unit are bridged by the two phenolate oxygens of the macrocyclic ligand and each of the metal ions have N_2O_2 equatorial planes, of which the larger ligand compartment is occupied by the vanadium. Both the metal centers obtain distorted octahedral geometry involving the *transoid* linkages O(1)−V(1)−O(7) and OW(1)−Ni−O(4). The in-plane V(1)−O and V(1)−N distances are normal, as is the distance V(1)=O(1), 1.607(6) Å; however, the V(1)−O(7) distance, 2.207(5) Å, is significantly long due to the *trans* effect of the V=O moiety. Tetragonally elongated geometry for the nickel(II) center is evident from the relatively long Ni−OW(1) distance (2.191(8) Å) and Ni−O(4) distance (2.140(6) Å). The equatorial Ni−O and Ni−N distances are compatible with the high-spin configuration since these are longer compared to their counterparts in the low-spin situation.[20] $\{(VO)L^2Ni(H_2O)\}$ unit is of convex shape when viewed down the V=O(1) and Ni—OW(1) bonds. This may be realized by considering the displacements of the metal centers and phenolate oxygens, all in the same direction, from an exact plane formed by the four amine nitrogens: Ni, 0.22 Å; V(1), 0.53 Å; O(2), 0.69 Å; O(3), 0.32 Å. In this context it may be noted that while the nickel atom is only slightly displaced (0.02 Å) from its O(2)O(3)N(3)N(4) basal plane, the vanadium atom is pushed toward O(1) by about 0.32 Å from its N(1)N(2)O(2)O(3) equatorial plane; these equatorial planes are inclined to each other by 20.1°. Furthermore, the two metal centers are separated by 3.006(2) Å with the Ni−O−V bridge angles of 96.7(3) and 98.8(3)°.

In the mononuclear $\{(VO_2)(HL^2)\}$ unit the vanadium atom

(31) Bradford, S. G.; Edelstein, N.; Hawkins, C. J.; Shalimoff, G.; Snow, M. R.; Tiekink, R. T. *Inorg. Chem.* **1990**, *29*, 434.
(32) Li, X.; Lah, M. S.; Pecoraro, V. L. *Inorg. Chem.* **1988**, *27*, 4657.
(33) Kojima, A.; Okazaki, K.; Ooi, S.; Saito, K. *Inorg. Chem.* **1983**, *22*, 1168.
(34) Drew, R. E.; Einstein, F. W. B.; Gransden, S. E. *Can. J. Chem.* **1974**, *52*, 2184.
(35) (a) Scheidt, W. R.; Tsai, C.; Hoard, J. L. *J. Am. Chem. Soc.* **1971**, *93*, 3867. (b) Scheidt, W. R.; Collins, D. M.; Hoard, J. L. *J. Am. Chem. Soc.* **1971**, *93*, 3873. (c) Scheidt, W. R.; Countryman, R.; Hoard, J. L. *J. Am. Chem. Soc.* **1971**, *93*, 3878.
(36) (a) Takaguchi, H.; Isobe, K.; Nakamura, Y.; Kawaguchi, S. *Bull. Chem. Soc. Jpn.* **1978**, *51*, 2030. (b) Riechel, T. L.; Sawyer, D. T. *Inorg. Chem.* **1975**, *14*, 1869.
(37) (a) Nishizawa, M.; Hirotsu, K.; Ooi, S.; Saito, K. *J. Chem. Soc., Chem. Commun.* **1979**, 707. (b) Kojima, A.; Okazaki, K.; Ooi, S.; Saito, K. *Inorg. Chem.* **1983**, *22*, 1168.
(38) Abbreviations: nta^{3-} = nitrilotriacetate; $peida^{2-}$ = (*S*)-[[1-(2-pyridyl)-ethyl]imino]diacetate.
(39) (a) Müller, A.; Penk, M.; Krichemeyer, E.; Bogge, H.; Walberg, H.-J. *Angew. Chem., Int. Ed. Engl.* **1988**, *27*, 1719. (b) Müller, A.; Rohlfing, R.; Doring, J.; Penk, M. *Angew. Chem., Int. Ed. Engl.* **1991**, *30*, 588.
(40) (a) Chen, Q.; Goshorn, D. P.; Scholes, C. P.; Tan, X.; Zubieta, J. *J. Am. Chem. Soc.* **1992**, *114*, 4667. (b) Khan, M. I.; Chen, Q.; Goshorn, D. P.; Zubieta, J. *Inorg. Chem.* **1993**, *32*, 672. (c) Khan, M. I.; Chen, Q.; O'Connor, C. J.; Zubieta, J. *Inorg. Chem.* **1993**, *32*, 2929. (d) Khan, M. I.; Lee, Y.-S.; O'Connor, C. J.; Zubieta, J. *J. Am. Chem. Soc.* **1994**, *116*, 5001.

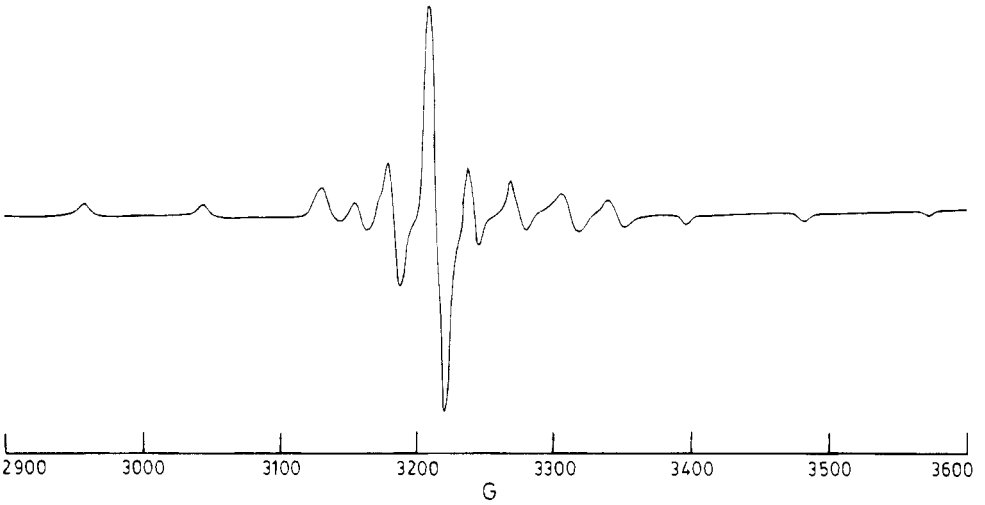

Figure 2. EPR spectrum of $[NiL^2(VO)(SO_4)]\cdot H_2O$ (**10**) in frozen $CH_2Cl_2-CH_3OH$ glass at 77 K. Microwave frequency: 9.112 GHz.

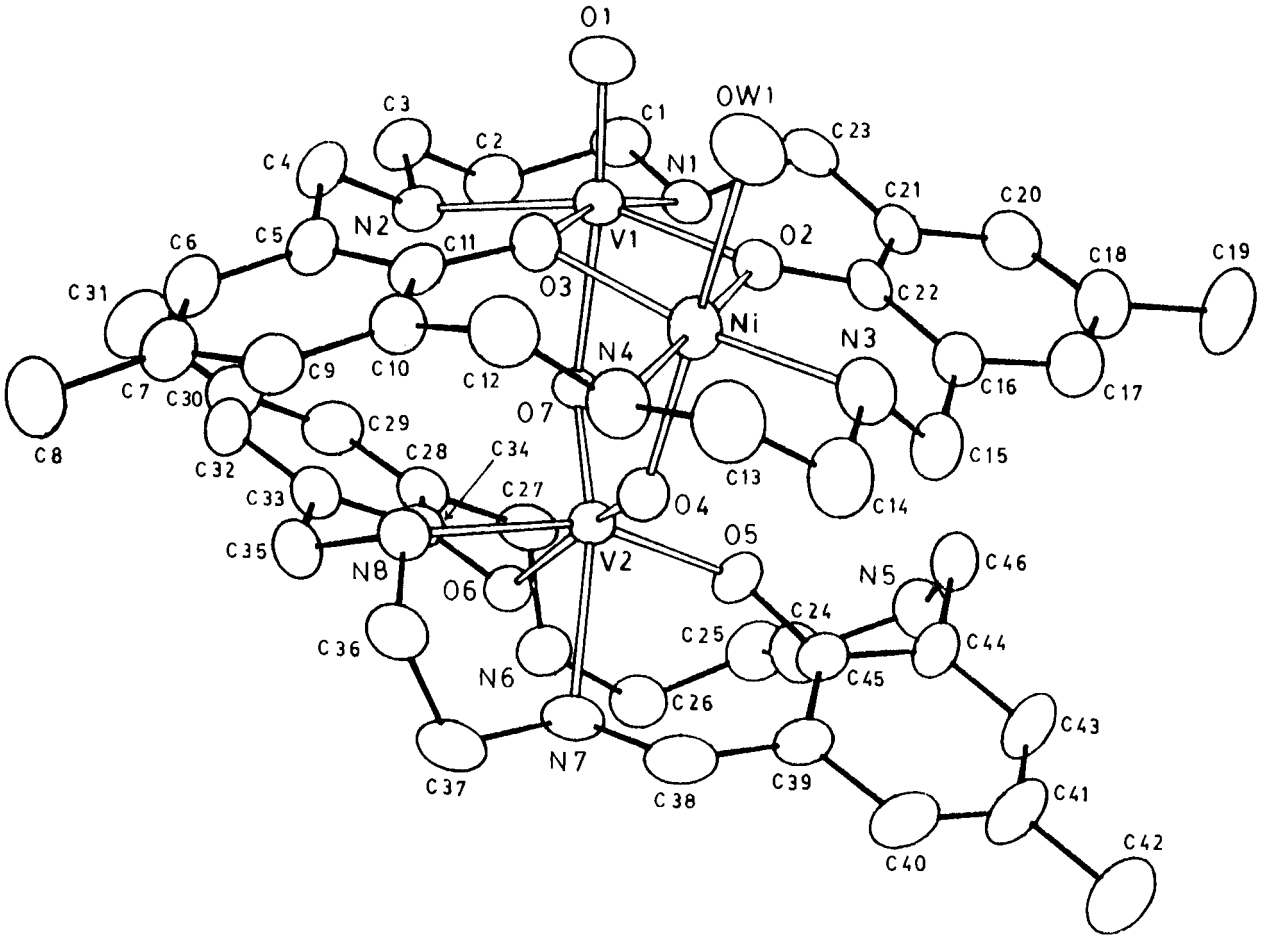

Figure 3. ORTEP view of $[\{(VO)L^2Ni(H_2O)\}\{(VO_2)(HL^2)\}]^{2+}$ cation in **5**.

occupies the smaller ligand compartment, while the empty larger ligand compartment adopts a folded configuration with one of its amine nitrogens protonated. The coordination environment of V(2), is *cis*-dioxo (O(4), O(7)) octahedral, which is displaced from its basal plane, N(7)N(8)O(5)O(7), toward one of the oxo groups (O(4)) by 0.18 Å. The V=O distances (1.658(5) and 1.650(6) Å) are within the range, 1.61−1.68 Å, reported for a number of structurally characterized complexes where the vanadyl oxygens are involved in bridges.[31−35] The *cis*-dioxo O(4)V(2)O(7) angle, 101.3(3)°, is slightly less kinked than the reported OVO angles[31−35] lying between 103.5 and 107.5°. The V(2)−O(6) distance (2.110(6) Å) and V(2)−N(7) distance (2.254(7) Å) are considerably longer than the other two pairs (1.865(5) and 2.158(7) Å), again showing a significant *trans* effect of both the V=O groups. The hetero-dinuclear $\{(VO)L^2Ni(H_2O)\}$ and mononuclear $\{(VO_2)(HL^2)\}$ units are anchored by the VO_2 oxygens, the V(2)O(7)V(1) and V(2)O(4)Ni bridge angles begin 137.6(3)° and 132.6(3)°, respectively.

Mixed-valence vanadium complexes formed as adducts between vanadium(IV) and vanadium(V) complexes have been reported in the literature.[36] However, none of these compounds have been structurally characterized. Concerning the dinuclear complexes we are aware of two mixed-valence complexes with V_2O_3 cores, viz. $(NH_4)_3[V^{IV}O(nta)-O-V^{V}O(nta)]\cdot 3H_2O$[37,38] and $Na[V^{IV}O(peida)-O-V^{V}O(peida)]\cdot NaClO_4\cdot H_2O$,[37,38] whose crystal structures have been determined. Recently, the electrochemical generation of a mixed-valence $[V^{IV}OL-O-V^{V}OL]^-$ (H_2L = 2,2-dihydroxyazobenzene) species in solution has been

Table 3. Fractional Atomic Coordinates[a] and Equivalent Isotropic Thermal Parameters U_{eq} (Å^2)[b] of the Non-Hydrogen Atoms for **5**

atom	*x*	*y*	*z*	U_{eq}	atom	*x*	*y*	*z*	U_{eq}
V(1)	0.65820(8)	0.62183(10)	0.15636(6)	0.0391(4)	C(20)	0.7146(6)	0.7037(7)	0.3430(4)	0.061(3)
V(2)	0.77745(8)	0.42791(9)	0.18922(5)	0.0340(4)	C(21)	0.6947(5)	0.6775(6)	0.2898(4)	0.047(2)
Ni	0.57420(8)	0.46829(10)	0.20162(6)	0.0475(4)	C(22)	0.6581(5)	0.5957(6)	0.2788(3)	0.040(2)
Cl(1)	0.2567(1)	0.0213(2)	0.6389(1)	0.0649(7)	C(23)	0.7096(5)	0.7420(6)	0.2472(4)	0.047(2)
Cl(2)	0.0555(1)	0.2482(2)	0.7000(1)	0.0622(7)	C(24)	0.9914(6)	0.4920(6)	0.3075(4)	0.058(3)
O(1)	0.6006(4)	0.7048(4)	0.1415(3)	0.056(2)	C(25)	1.0683(6)	0.5359(7)	0.2954(4)	0.061(3)
O(2)	0.6333(3)	0.5760(4)	0.2270(2)	0.042(1)	C(26)	1.1055(6)	0.4942(6)	0.2492(4)	0.056(3)
O(3)	0.5859(3)	0.5225(4)	0.1291(2)	0.044(1)	C(27)	1.0126(5)	0.5713(6)	0.1761(4)	0.049(2)
O(4)	0.6859(3)	0.3982(4)	0.2021(2)	0.042(1)	C(28)	0.9628(5)	0.5519(6)	0.1231(4)	0.046(2)
O(5)	0.8259(3)	0.4379(4)	0.2600(2)	0.042(1)	C(29)	0.9720(6)	0.5988(7)	0.0769(4)	0.057(3)
O(6)	0.8962(3)	0.4367(4)	0.1667(2)	0.039(1)	C(30)	0.9270(6)	0.5831(7)	0.0287(4)	0.060(3)
O(7)	0.7615(3)	0.5306(3)	0.1692(2)	0.034(1)	C(31)	0.9375(7)	0.6365(9)	−0.0220(5)	0.084(4)
O(8)	0.3108(5)	−0.0493(5)	0.6351(4)	0.094(3)	C(32)	0.8722(6)	0.5136(7)	0.0280(4)	0.059(3)
O(9)	0.2702(6)	0.0854(6)	0.5982(4)	0.102(3)	C(33)	0.8610(5)	0.4638(6)	0.0720(4)	0.046(2)
O(10)	0.1759(4)	−0.0102(5)	0.6305(3)	0.085(2)	C(34)	0.9066(5)	0.4829(6)	0.1224(4)	0.042(2)
O(11)	0.2713(5)	0.0615(6)	0.6908(3)	0.097(3)	C(35)	0.8131(6)	0.3816(7)	0.0682(4)	0.052(2)
O(12)	0.0976(4)	0.3216(4)	0.7256(3)	0.072(2)	C(36)	0.7331(6)	0.2770(6)	0.1152(4)	0.052(2)
O(13)	0.1116(5)	0.1869(5)	0.6828(4)	0.093(3)	C(37)	0.8012(6)	0.2346(6)	0.1515(4)	0.059(3)
O(14)	0.0064(4)	0.2076(5)	0.7369(3)	0.082(2)	C(38)	0.7832(6)	0.2491(6)	0.2476(4)	0.058(3)
O(15)	0.0051(5)	0.2801(5)	0.6540(3)	0.083(2)	C(39)	0.8052(5)	0.2964(6)	0.2995(4)	0.045(2)
N(1)	0.7446(4)	0.7019(4)	0.1999(3)	0.042(2)	C(40)	0.8052(6)	0.2486(7)	0.3485(5)	0.062(3)
N(2)	0.7111(4)	0.6245(5)	0.0822(3)	0.042(2)	C(41)	0.8239(7)	0.2849(8)	0.3981(4)	0.069(3)
N(3)	0.5523(4)	0.4280(6)	0.2757(3)	0.055(2)	C(42)	0.8216(8)	0.2314(9)	0.4482(5)	0.099(4)
N(4)	0.5234(4)	0.3570(5)	0.1730(3)	0.056(2)	C(43)	0.8455(6)	0.3721(7)	0.4001(4)	0.061(3)
N(5)	0.9587(5)	0.5308(5)	0.3552(3)	0.057(2)	C(44)	0.8459(5)	0.4223(6)	0.3540(3)	0.046(2)
N(6)	1.0503(4)	0.4885(5)	0.1976(3)	0.048(2)	C(45)	0.8251(5)	0.3846(6)	0.3031(4)	0.043(2)
N(7)	0.8184(4)	0.2878(4)	0.2012(3)	0.047(2)	C(46)	0.8698(6)	0.5174(6)	0.3584(4)	0.052(2)
N(8)	0.7532(4)	0.3722(5)	0.1095(3)	0.044(2)	OW(1)	0.4628(4)	0.5454(5)	0.2008(3)	0.082(2)
C(1)	0.7791(6)	0.7716(6)	0.1672(4)	0.050(2)	OW(2)[a]	0.3121(24)	−0.0174(25)	0.8016(16)	0.249(15)
C(2)	0.8114(6)	0.7377(6)	0.1175(4)	0.056(3)	OW(2)A[a]	0.3882(31)	−0.0157(33)	0.8069(20)	0.348(22)
C(3)	0.7491(6)	0.7090(6)	0.0705(4)	0.053(2)	OW(3)[a]	0.5544(16)	0.8725(17)	0.1031(11)	0.162(9)
C(4)	0.6511(6)	0.5990(6)	0.0353(3)	0.050(2)	OW(3)A[b]	0.5618(27)	0.8569(30)	0.0694(18)	0.145(15)
C(5)	0.6183(5)	0.5065(6)	0.0381(3)	0.047(2)	OW(3)B[b]	0.5797(20)	0.8989(22)	0.1360(13)	0.1007(10)
C(6)	0.6192(6)	0.4537(7)	−0.0068(4)	0.053(3)	OW(4)[a]	0.4897(17)	0.6516(18)	0.3876(11)	0.172(10)
C(7)	0.5829(6)	0.3725(7)	−0.0106(4)	0.057(3)	OW(4)A[a]	0.4150(13)	−0.1376(14)	0.7977(8)	0.135(7)
C(8)	0.5843(7)	0.3159(8)	−0.0593(4)	0.078(3)	OM(1)[c]	1.0934(12)	0.4656(12)	0.4602(7)	0.135(6)
C(9)	0.5409(6)	0.3481(6)	0.0318(4)	0.053(2)	OM(1)A[d]	1.0564(13)	0.4263(14)	0.4289(9)	0.095(6)
C(10)	0.5367(5)	0.3969(6)	0.0778(4)	0.048(2)	CM(1)[c]	1.0238(21)	0.5184(24)	0.4625(16)	0.177(15)
C(11)	0.5805(5)	0.4772(6)	0.0827(4)	0.046(2)	CM(1)A[d]	1.0627(32)	0.4356(37)	0.4840(14)	0.159(20)
C(12)	0.4807(6)	0.3685(7)	0.1188(4)	0.063(3)	OM(2)[a]	0.7453(12)	0.4794(13)	0.5610(8)	0.110(6)
C(13)	0.4751(6)	0.3252(8)	0.2153(4)	0.071(3)	OM(2)A[b]	0.8038(25)	0.4582(27)	0.5475(16)	0.128(13)
C(14)	0.5286(6)	0.3343(7)	0.2689(4)	0.068(3)	OM(2)B[b]	0.7284(23)	0.4990(25)	0.5827(15)	0.106(11)
C(15)	0.6227(6)	0.4431(7)	0.3157(4)	0.059(3)	CM(2)[a]	0.6984(31)	0.4214(33)	0.5194(19)	0.242(22)
C(16)	0.6481(5)	0.5377(6)	0.3216(3)	0.046(2)	CM(2)A[b]	0.7931(57)	0.5475(37)	0.5679(36)	0.201(36)
C(17)	0.6680(7)	0.5677(8)	0.3740(4)	0.065(3)	CM(2)B[b]	0.6794(68)	0.4255(76)	0.5589(45)	0.236(44)
C(18)	0.6993(7)	0.6502(8)	0.3860(4)	0.070(3)	OM(3)[a]	0.5360(21)	0.0932(24)	0.0138(14)	0.215(13)
C(19)	0.7200(10)	0.6795(9)	0.4435(4)	0.103(5)	CM(3)[a]	0.5442(37)	0.0519(39)	−0.0378(20)	0.233(25)

[a] Site occupancy: a = 0.50, b = 0.25, c = 0.60, and d = 0.40. [b] U_{eq} is defined as one-third of the trace of the orthogonalized $\mathbf{U}_{ij}$ tensor.

reported,[15a] that exhibits 15-line EPR spectrum in fluid at room temperature due to delocalization of the odd electron over the two metal centers. Compared to the dinuclear systems a variety of well-characterized mixed-valence $V^{IV}V^{V}$ species have been reported for polyoxovanadium[39] and polyoxoalkoxovanadium[40] clusters. They provide examples of novel structural motifs where the metal centres in the clusters can be oxidized or reduced. The hetero-trinuclear complex reported here presents yet another type of stable mixed-valence $V^{IV}V^{V}$ species.

Electrochemistry. The cyclic voltammograms for complexes **6**, **8**, **9**, and **10** with regard to their oxidation behavior in MeCN−MeOH (2:1) solutions using platinum electrodes are shown in Figure 4. All the complexes undergo one electron oxidation, $V^{IV}O \rightarrow V^{V}O$, whose redox potentials and heterogeneous electron transfer rates show dependence on the coordinating ability of the anions, but not on the presence of the neighboring nickel(II) ion. For example, both $[(VO)H_2L^2(SO_4)]$ (**8**) and $[NiL^2(VO)(SO_4)]$ (**10**) get reversibly oxidized at the same potential ($E_{1/2}$ = 0.57 V vs Ag/AgCl) with the identical difference in peak potentials (ΔE_p = 65 mV) that remains invariant with change of scan rates. Similarly, the $E_{1/2}$ values of **9** (0.79 V) and **6** (0.80 V) are almost the same, albeit their electron transfer rates differ (ΔE_p = 90 mV for **9** and 150 mV for **6** at v = 100 mV s^{-1}). Thus, the low-spin nickel(II) plays a spectator role in the redox process when oxovanadium(IV) occupies the larger ligand compartment. On the other hand, the oxidation of vanadium(IV) is considerably facilitated by the coordinated electron-rich sulfate as against the noncoordinated nitrate or perchlorate anions. In contrast to **6**, the positional isomer **4** is not electroactive in the potential window 0−1 V, indicating that when oxovanadium(IV) occupies the smaller ligand compartment, it is far more reluctant to get oxidized. This shows that Ni^{2+} ion is ineffective to augment aerial oxidation of VO^{2+} to VO_2^+ ion. Clearly, the formation of **5** is antecedent to the generation of **3** in the insoluble mixture. Finally, we note that **5** irreversibly gets oxidized at 0.85 V.

Magnetic Properties. The variable-temperature (80−293 K) magnetic susceptibility data were collected for complexes **4**, **5**, and **7**. The χ_M vs T values for **4** and **7** are illustrated in Figure 5. The effective magnetic moments for all the complexes at room temperature indicate a total spin of $S = {}^3/_2$ due to the high-spin nickel(II) ($S_1 = 1$) and oxovanadium(IV) ($S_2 = {}^1/_2$). It may be noted in Figure 5 that the χ_M values increase slowly with the decrease of temperature. A similar trend with even slower rate of decrease of $\chi_M T$ with the increase of temperature was noted in $\chi_M T$ vs T plots, indicating weak ferromagnetic

Table 4. Selected Bond Distances (Å) and Angles (deg) for $[\{(VO)L^2Ni(H_2O)\}\{(VO_2)HL^2\}](ClO_4)_2 \cdot 3H_2O \cdot 2.5CH_3OH$ (**5**)

V(1)−N(1)	2.099(7)	Ni−N(3)	2.011(8)	V(2)−N(7)	2.254(7)
V(1)−N(2)	2.124(7)	Ni−N(4)	1.996(8)	V(2)−N(8)	2.158(7)
V(1)−O(1)	1.607(6)	Ni−OW(1)	2.191(8)	V(2)−O(4)	1.650(6)
V(1)−O(2)	1.975(6)	Ni−O(2)	1.985(6)	V(2)−O(5)	1.865(5)
V(1)−O(3)	2.009(6)	Ni−O(3)	2.013(6)	V(2)−O(6)	2.110(6)
V(1)−O(7)	2.207(5)	Ni−O(4)	2.140(6)	V(2)−O(7)	1.658(5)

N(1)−V(1)−N(2)	96.6(3)	OW(1)−Ni−O(2)	87.0(3)
N(1)−V(1)−O(1)	91.1(3)	OW(1)−Ni−O(3)	86.0(3)
N(1)−V(1)−O(2)	86.7(3)	OW(1)−Ni−O(4)	177.5(3)
N(1)−V(1)−O(3)	165.3(3)	O(3)−Ni−O(4)	92.7(2)
N(1)−V(1)−O(7)	79.2(2)	N(7)−V(2)−N(8)	76.9(3)
N(2)−V(1)−O(1)	94.3(3)	N(7)−V(2)−O(4)	89.1(3)
N(2)−V(1)−O(2)	157.4(3)	N(7)−V(2)−O(5)	81.8(3)
N(2)−V(1)−O(3)	90.4(3)	N(7)−V(2)−O(6)	79.5(2)
N(2)−V(1)−O(7)	75.7(2)	N(7)−V(2)−O(7)	166.8(3)
O(1)−V(1)−O(2)	108.1(3)	N(8)−V(2)−O(4)	89.0(3)
O(1)−V(1)−O(3)	101.3(3)	N(8)−V(2)−O(5)	157.2(3)
O(1)−V(1)−O(7)	165.0(3)	N(8)−V(2)−O(6)	82.6(3)
O(2)−V(1)−O(3)	82.0(2)	N(8)−V(2)−O(7)	95.1(3)
O(2)−V(1)−O(7)	83.0(2)	O(4)−V(2)−O(5)	99.0(3)
O(3)−V(1)−O(7)	90.1(2)	O(4)−V(2)−O(6)	167.1(3)
N(3)−Ni−N(4)	87.5(3)	O(4)−V(2)−O(7)	101.3(3)
N(3)−Ni−OW(1)	86.6(3)	O(5)−V(2)−O(6)	85.5(2)
N(3)−Ni−O(2)	95.3(3)	O(5)−V(2)−O(7)	104.2(3)
N(3)−Ni−O(3)	172.1(3)	O(6)−V(2)−O(7)	89.2(3)
N(3)−Ni−O(4)	94.6(3)	V(1)−O(2)−Ni	98.8(3)
N(4)−Ni−OW(1)	97.4(3)	V(1)−O(3)−Ni	96.7(3)
N(4)−Ni−O(2)	175.9(3)	V(1)−O(7)−V(2)	137.6(3)
N(4)−Ni−O(3)	96.1(3)	Ni−O(4)−V(2)	132.6(3)
N(4)−Ni−O(4)	84.9(3)		

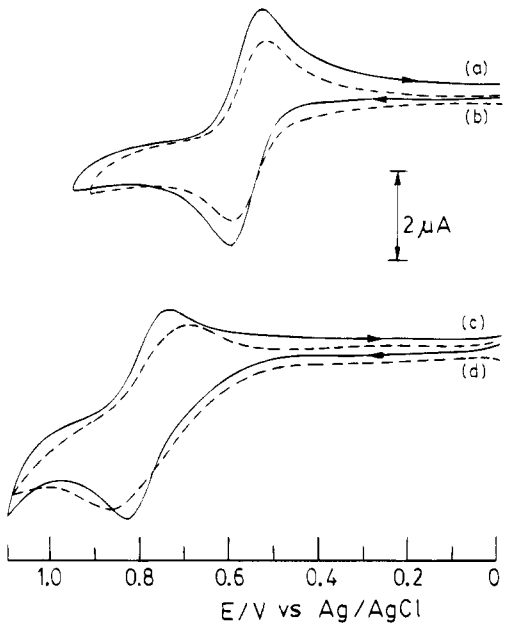

Figure 4. Cyclic voltammograms for **8** (a), **10** (b), **9** (c), and **6** (d) in MeCN−MeOH (2:1) solutions using Pt electrodes at a scan rate of 100 mV s^{-1}. Concentrations of electroactive species were as follows: **8** (1.02 mM); **10** (0.96 mM); **9** (1.08 mM); **10** (1.10 mM).

exchange interaction in all these cases. Assuming an isotropic model, the exchange expression based on the spin Hamiltonian $\mathbf{H} = -2J\mathbf{S}_1 \cdot \mathbf{S}_2$ is given by

$$\chi_M = \frac{N\beta^2 g^2}{4kT}\left[\frac{1 + 10\exp(3J/kT)}{1 + 2\exp(3J/kT)}\right] \quad (2)$$

The symbols N, β, g, and k have their usual meanings. Since the measurement was limited up to 80 K, additional terms due to temperature-independent paramagnetism and contribution of mononuclear paramagnetic impurity were not considered. Moreover, no attempt was made to include zero-field splitting

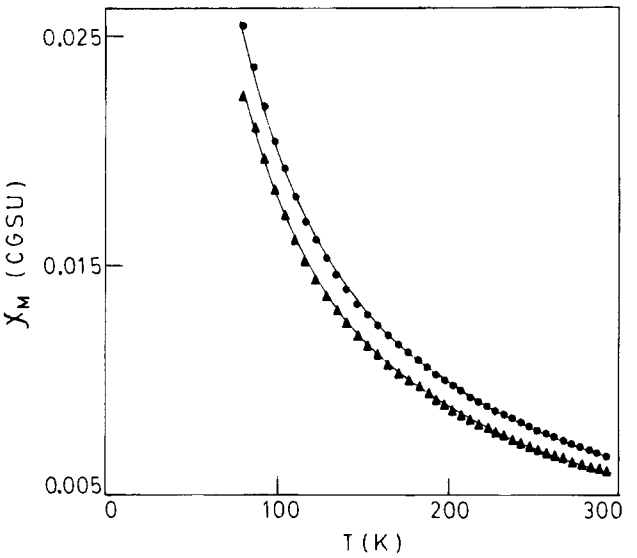

Figure 5. Molar magnetic susceptibility (χ_M) per complex molecule vs temperature (T) for **4** (●) and **7** (▲). The solid lines result from a least-squares fit to the theoretical eq 2 given in the text.

Table 5. Magnetic Data for the Complexes

complex	J, cm^{-1}	g	10^2R^a
$[(VO)L^2Ni(H_2O)_2](ClO_4)_2$ (**4**)	12	2.30	2.5
$[\{(VO)L^2Ni(H_2O)\}\{(VO_2)HL^2\}](ClO_4)_2 \cdot 3H_2O \cdot 2.5CH_3OH$ (**5**)	2	2.26	2.2
$[(VO)L^2Ni(py)](ClO_4)_2 \cdot H_2O$ (**7**)	5	2.25	0.69

^{a} $R = [\sum((\chi_m(\text{obsd}) - \chi_m(\text{calcd}))^2/\sum\chi_M(\text{obsd})^2]^{1/2}$.

parameter of nickel(II) ion, whose contribution is significant only at the low temperature region.

Least-squares fitting of eq 2 to the experimental data for complexes **4** and **7** is shown in Figure 5. The relevant magnetic parameters thus obtained are given in Table 5. Although singlet ground states have been reported for a fairly large number of dioxovanadium(IV) complexes[41] having phenoxo, alkoxo, hydroxo, or oxo bridges, only few of them[17,19,42,43] can be subjected to scrutiny for magnetostructural relationships. In general, the reported antiferromagnetic spin exchange coupling constants ($-J$) are moderate to strong; however, in a monooxo bridged complex[43] the $-J$ value has been found to be as high as 500 cm^{-1}. Since in these compounds the unpaired electron on each of the oxovanadium center resides on d_{xy} orbital, a through space, direct overlap of d_{xy} orbitals (π-interaction) is considered as the dominant magnetic exchange pathway in contrast to the superexchange that occurs through the σ-backbone involving $d_{x^2-y^2}$ orbitals, as in dicopper(II) or dinickel(II) complexes.

As yet, magnetic properties of heteronuclear oxovanadium(IV) complexes have received scant attention. The most well-known and best studied system in $[VO(fsa)_2enCu] \cdot CH_3OH$[44] ($H_4$(fsa)en = *N*,*N*′-(2-hydroxy-3-carboxybenzilidine)ethylenediamine). In this compound the molecular symmetry allows to achieve strict orthogonality of the magnetic orbitals of the two

(41) (a) Dutton, J. C.; Murray, K. S.; Tiekink, E. R. *Inorg. Chim. Acta* **1989**, *166*, 5. (b) Julve, M.; Verdaguer, M.; Charlot, M.-F.; Kahn, O.; Claude, R. *Inorg. Chim. Acta* **1984**, *82*, 5. (c) Heeg, M. J.; Mack, J. L.; Glick, M. D.; Lintvedt, R. L. *Inorg. Chem.* **1981**, *20*, 833. (d) Okawa, H.; Audo, I.; Kida, S. *Bull. Chem. Soc. Jpn.* **1974**, *47*, 3041. (e) Ozarowski, A.; Reinen, D. *Inorg. Chem.* **1986**, *25*, 1704. (f) Ginsberg, A. P.; Koubeck, E.; Williams, H. J. *Inorg. Chem.* **1966**, *5*, 1656.
(42) Neves, A.; Wieghardt, K.; Nuber, B.; Weiss, J. *Inorg. Chim. Acta* **1988**, *150*, 183.
(43) Tofflund, H.; Larsen, S.; Murray, K. S. *Inorg. Chem.* **1991**, *30*, 3964.
(44) (a) Kahn, O.; Galy, J.; Journaux, Y.; Morgenstern-Badarau, I. *J. Am. Chem. Soc.* **1982**, *104*, 2165. (b) Loth, P. de; Karafiloglou, P.; Daudey, J. P.; Kahn, O. *J. Am. Chem. Soc.* **1988**, *110*, 5676.

metal centers viz. d_{xy} and $d_{x^2-y^2}$ orbitals. As a result, the compound behaves strongly ferromagnetically ($2J = 118\ cm^{-1}$) with the triplet ground state.

In complexes **4**, **5**, and **7**, the steric environment around nickel is either octahedral or square pyramidal. Since both of the magnetic orbitals of nickel ($d_{x^2-y^2}$ and d_{z^2}) are orthogonal to that of vanadium (d_{xy}), an overall ferromagnetic interaction is expected. However, as has been pointed out[44b] the singlet–triplet energy gap is affected inter alia by symmetry of the molecular species and the interacting magnetic orbitals as a whole, spin polarization and charge transfer phenomenon. We note that although the decreasing ferromagnetic order **4** > **7** > **5** presents an interesting trend, rationalization of this behavior should wait till the structural results are available. A detailed study on related copper(II)–oxovanadium(IV) systems are underway and will be the subject of a future report.

Acknowledgment. Financial assistance received from the SERC of the Department of Science & Technology, Government of India is gratefully acknowledged. We are thankful to Dr. P. Chaudhuri of Ruhr University, Bochum for variable-temperature magnetic measurements.

Supplementary Material Available: Tables of anisotropic thermal parameters, hydrogen atom positions, complete of bond distances and angles, and hydrogen bond distances and angles for complex **5** (9 pages). Ordering information is given on any current masthead page.

IC9408819